Journal of Renewable Materials

Tech Science Press

DOI: 10.32604/jrm.2022.019270

ARTICLE

Hydrophobic Poplar Prepared via High Voltage Electric Field (HVEF) with Copper as Electrode Plate

Jianxin Cui[1,#], Zehui Ju[1,#], Lu Hong[2], Biqing Shu[1,3] and Xiaoning Lu[1,*]

[1]College of Materials Science and Engineering, Nanjing Forestry University, Nanjing, 210037, China

[2]School of Forestry and Landscape Architecture, Anhui Agricultural University, Hefei, 230036, China

[3]College of Civil Engineering, Yangzhou Polytechnic Institute, Yangzhou, 225127, China

[*]Corresponding Author: Xiaoning Lu. Email: luxiaoning-nfu@126.com

[#]These authors are contributed equally to this work

Received: 13 September 2021 Accepted: 24 November 2021

ABSTRACT

In order to improve hydrophobic characteristics which will affect the service performance of fast-growing poplar due to growing bacteria in the humid environment. In this study, a simple method was proposed to treat poplar via the high voltage electric field (HVEF) with copper as the electrode plate. Scanning electron microscope (SEM), Fourier transforms infrared spectroscopy (FTIR), X-ray diffraction (XRD) and contact angle tester were adopted to evaluate the surface morphology, surface group of poplar, crystallinity and wettability under HVEF. It was found by SEM that a large number of copper particles were uniformly attached to the surface of poplar. In all three sections, the weight percentage of the Cu element was accounting for more than half. The diffraction peaks of copper-containing compounds appeared in the (XRD). FTIR analysis confirmed that the reaction between copper and poplar took place. The surface contact angle of three sections of poplar increased in the following order: cross section < radial section < tangential section (increased by 34°, 45° and 53°, respectively). An environment-friendly and efficient method of HVEF treating fast-growing wood with copper as the electrode plate can promote its outdoor application.

KEYWORDS

Poplar; high voltage electric field; wettability; hydrophobic; copper particles

1 Introduction

As a kind of economical wood, poplar has the characteristics of fast-growing and environmental protection, and it has been widely used in various fields [1]. However, poplar is easy to absorb moisture, especially in a humid environment, which can cause bacteria to grow on the surface of the wood, accumulate impurities and dirt, etc., and which will eventually deform or mildew [2,3]. In recent years, Many physical [4,5], chemical [6–8], biological [9] or mechanical [10] methods have been used to improve the performance of poplar in harsh environments.

The hydrophobic surface has the characteristics of self-cleaning and anti-pollution, so improving the hydrophobicity of the wood surface can effectively improve its performance under high humidity conditions. Wood is a porous structural material with micron-level pore diameters and has a natural

micron-level surface roughness. Therefore, to obtain a super-hydrophobic surface for wood, theoretically only need to construct a nano-scale structure and reduce surface energy treatment can be achieved [11,12]. At present, the main methods are sol-gel method [13], hydrothermal method [14], plasma technology [15,16], chemical vapor deposition method [17,18] and so on. Yang et al. [19] prepared core-shell particles by infiltrating silica and polystyrene into the hollow microspheres. The ethanol dispersion of core-shell particles was sprayed onto the epoxy-treated wood surface in different proportions. The contact angle of treated wood is around 150°. Wang et al. [20] used rose petals as a template, polydimethylsiloxane (PDMS), and different concentrations of polyvinyl alcohol (PVA) as reagents. The research adopted the stencil printing method, and after the second replication, it has the same characteristics as roses. The results show that the contact angle of wood is increased from 59.25° to more than 140° after bionics, which has hydrophobic properties similar to rose petals. Song et al. [21] build hydrophobicity and resistance to damage to the wood surface through the reaction of hydroxyl with metal ions. The original woodblock is immersed in a salt solution and then dried, and the surface of the treated wood shows a better hydrophobic behavior. The surface of Zr^{4+} ion-treated wood shows the best modification effect. The contact angle of radial direction is 145° and the cross section is 139°. Wang et al. [22] used the adhesion properties of polydopamine and chemical deposition to coat copper nanoparticles on the wood surface. The contact angle of the coating is about 157°, showing excellent chemical stability and antibacterial properties. Coating metal ions on the surface of wood by chemical means can improve the hydrophobic and antibacterial properties of wood. The cost of copper ions is lower than that of silver ions, so this study chooses copper ions to modify wood. However, the conditions of chemical processing are demanding, the cost is high, and it has a negative impact on the environment. Therefore, an environmentally friendly processing method is urgently needed.

High voltage electric field (HVEF) technology is widely used in the process of material manufacturing and modification due to its unique mechanism of action on the surface and interface of materials [23,24]. Ju et al. [25] studied the interaction mechanism of copper particles with hemicellulose and lignin in bamboo under different high-voltage electric field treatment conditions. The results show that the copper particles are present on the surface of treated bamboo in the form of different valences copper ions and copper oxide. As the treatment time and voltage intensity increase, the copper content on the surface of the bamboo increases. The size of the copper particles also increases. Also, the treated wood has excellent antibacterial and anti-ultraviolet functions. Furthermore, He et al. [26] studied the chemical characteristics and antifungal properties of poplar and other susceptible species under the HVEF treatment with silver as electrode plate particles. The silver particles reacted with polar groups on the surface of treated wood. Laboratory antifungal tests showed that the quality loss of treated samples decreased (<1%) after exposure to rotting fungi. The results indicate that the effect of silver particles and HVEF treatment can effectively enhance the antifungal properties of the poplar. In the existing HVEF research, metal ions are mainly loaded on wood to improve performance in various aspects [27,28], but few studies on the hydrophobic properties of the wood surface were reported. Our group has deep research in the treatment of wood with HVEF, so it is feasible to apply HVEF technology to improve the hydrophobic properties of wood. In addition, the high-voltage electrostatic treatment method is a pollution-free, low-cost and efficient treatment method.

This paper was to treat poplar via HVEF with copper as the electrode plate. Thereby changing the wettability of the poplar surface and making it a new type of hydrophobic material. The treatment of intensity with HVEF was optimized and the wettability of the three sections of poplar after the treatment of HVEF is studied.

2 Materials and Methods

2.1 Materials

The poplar wood was selected from the northern region of Jiangsu Province, China. The moisture content is about 10%, cut the sample with the size of 20 mm × 20 mm × 20 mm (longitudinal × radial × tangential), sand with 240 grit sandpaper until its surface roughness (Ra) is 2.8 μm, and use an air compressor to blow off the excess wood powder. The position of the sample is closer to the sapwood, and the sample has no defects. The size of the metal copper electrode plate is 150 mm × 150 mm × 1.5 mm (length × width × height).

2.2 High-Voltage Electric Field Treatment

First, the surface of poplar samples is clean and the copper plates are clean and smooth. The three sections of the poplar cubes are discharged in an orderly manner and exposed to HVEF (Fig. 1). The copper plate on the upper surface is connected to the electrostatic generation system as a negative electrode, and the copper plate on the lower surface is grounded as a positive electrode. The surface to be processed is contacted with the negative plate, and pressure of 0.1 MPa is applied to the copper plate to make the copper plate and the samples in close contact during the processing. To ensure the safety of the experiment, the outside of the upper and lower copper plates are insulated with the polytetrafluoroethylene (PTFE) sheet. The voltage of the high voltage device is 60 kV, the temperature is 40°C, the time is 24 h, and the pressure is controlled within the sample compression rate of 5%.

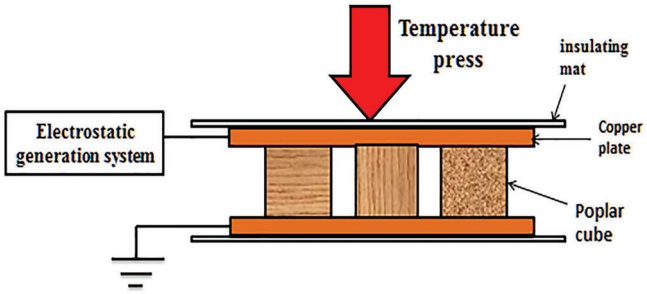

Figure 1: Schematic diagram of experimental set-up

2.3 Testing and Characterization

2.3.1 Observation of Surface Morphology and Elements Contents

Environmental scanning electron microscopy with EDS system (ESEM 200, FEI Co., Ltd., USA) was used to observe the surface morphology and the element content of poplar samples. Before ESEM/EDS experiments, the samples were baked in an oven at 100° for 8 h and sprayed the gold film on the sputtering device. The treated samples of three sections were cut into small blocks with treated surfaces. To determine the contents of the element of the samples, energy dispersion spectroscopy (EDS) analysis of the samples was adopted.

2.3.2 FTIR

Fourier transform infrared spectroscopy (Vertex 70 X type, German BRUKER Company, Germany) was used to analyze the changes of chemical groups before and after treatment of the three sections of poplar wood. The positive electrode surface layer of the poplar sample before and after the treatment was scraped and ground into 80 mesh wood powder for the test. The three sections only scrape the surface, and the inside of the block is not considered. The KBr compression method was adopted. The measuring range is 4000–400 cm^{-1} with a resolution of 4 cm^{-1}.

2.3.3 XRD

The D8 X-ray diffractometer (Bruker, Germany) was adopted to determine the surface chemical states and crystallinity of the poplar samples. The positive electrode surface layer of poplar samples before and after the treatment was scraped and ground into 80 mesh wood powder for the test. The three sections only scrape the surface, and the inside of the block is not considered. The scanning speed is 4°/min, the acceleration voltage is 40 kV, the current is 30 mA, and the range is 5–90°. The crystallinity of wood cellulose was calculated by the empirical method of Segal et al. [29]. As shown in Eq. (1):

$$C_rI\% = \frac{I_{002} - I_{am}}{I_{002}} \times 100\% \quad (1)$$

$C_rI\%$ is the relative crystallinity, I_{002} is the maximum intensity of the (002) lattice diffraction angle (near 22°), and I_{am} is the diffraction intensity of the amorphous region (near 18°).

2.3.4 Wettability

At room temperature, ultrapure (4 μL) water was used to test the water contact angle of the sample surface through the contact angle tester. The contact angle was tested immediately after the water droplets touched the sample surface. The five samples were tested and the average value represents the overall wettability of the poplar surface.

3 Results and Discussion

3.1 Surface Morphology and Elements Contents

Fig. 2 shows the surface morphology and elemental contents of treated poplar samples (cross section, tangential section and radial section). On untreated poplar surfaces, the cell walls are smooth and the lumen is empty on all three sections. After the treatment of HVEF, the covered copper particles can be seen on the poplar surface and form a rough surface. Some surfaces without copper particles may be caused by the fluctuation of voltage and time between the anode and cathode of copper plates in HVEF [30]. Gao et al. [31] fabricated a hydrophobic film containing cuprous oxide (Cu_2O) microspheres on a wooden substrate with a similar covering effect. The different structure distribution forms in the three sections have different effects on the coverage and reaction of the wood and copper particles. The distribution of tracheids or vessels can be seen on the cross section. And the different structural characteristics of the tube holes or tracheid channels, pits and wood rays can be observed on the tangential section and the radial section [32,33]. The presence of relatively large-sized vessels on the cross section causes the coverage of copper particles to be lower than that of the tangential section and the radial section. The microstructure of the tangential section and the radial section are closer, so the cover effect is similar.

The previous research has been reported that with the increase of processing voltage intensity and processing time, the size of copper particles attached to the surface increased and tended to be uniform. And the average size of copper particles was less than 60 nm [25]. Similar research mentioned electrospraying technique allows us to obtain particles with sizes less than 100 nm [33]. In view of the micron-level rough structure of the wood itself, the micro-nano level structure similar to the lotus leaf can be constructed after the uniformly distributed copper particles are loaded, which theoretically has the basic structural characteristics required for a superhydrophobic surface [34,35].

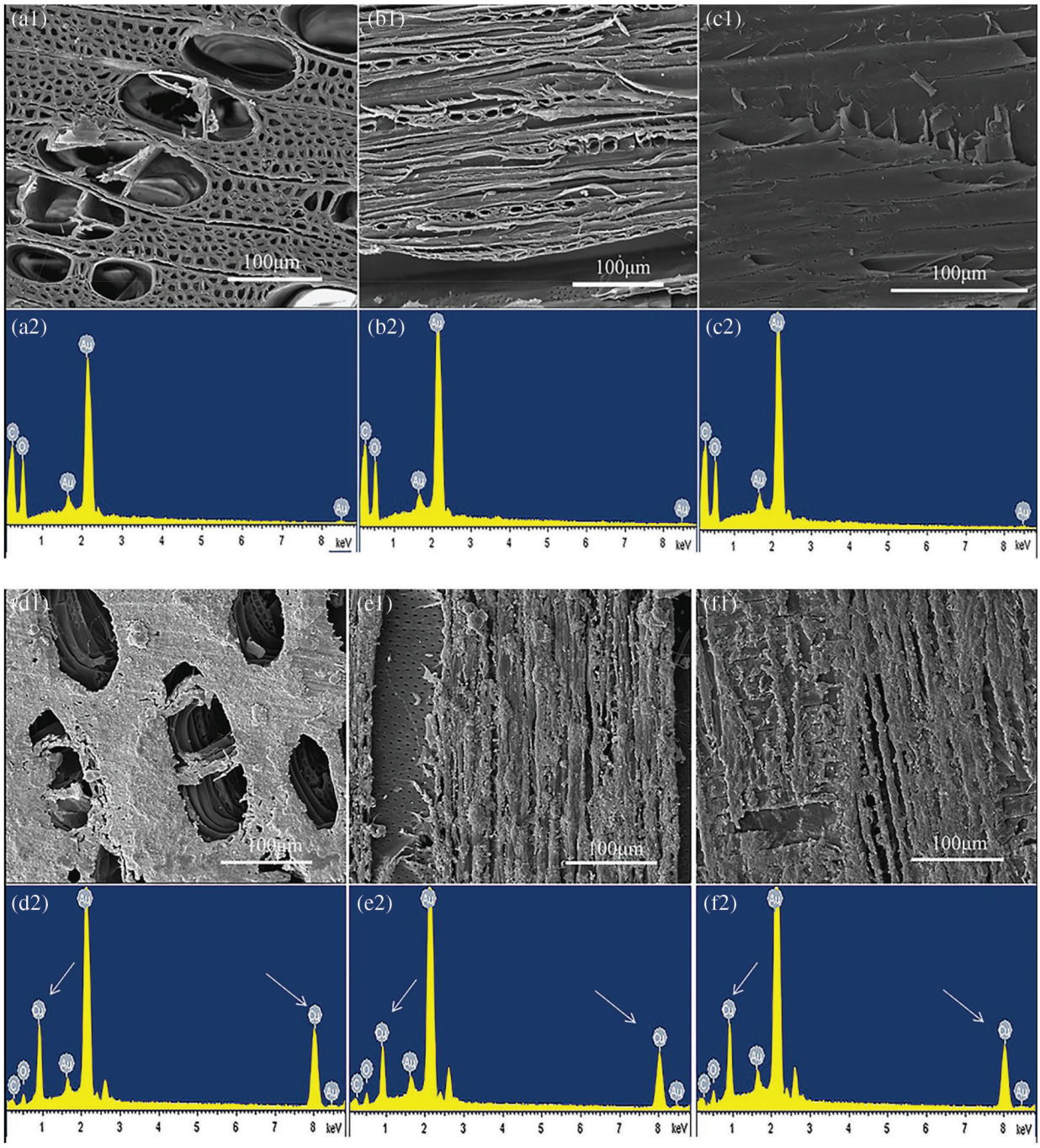

Figure 2: Surface morphology and elements contents of poplar samples: (1) SEM for three sections (cross section, tangential section and radial section) before (a1, b1, c1) and after (d1, e1, f1) treatment (60 kV) (2) Elements contents obtained by EDS for three sections before (a2, b2, c2) and after (d2, e2, f2) treatment (60 kV)

Table 1 shows the specific content of the element from EDS in three sections of the poplar surface. The element content analysis of the three sections is carried out in conjunction with the EDS diagram in Fig. 2. The results show that the content of C and O elements decreased and the Cu element increased. Among them,

C and O elements belong to the components of wood, the Au element comes from the conductive coating used for electron microscopy observation, and the Cu element is transmitted from the copper plate into the prepared sample. In all three sections, the content of Cu by weight accounts for more than half, while the proportions of C and O are respectively reduced to 10–15% of the total weight of the surface elements after treatment. Mu et al. covered more copper particles by controlling the processing time, and the weight percentage of Cu element in the EDS results can reach 86.12% [36]. Moreover, the copper content of the three sections is also slightly different. The copper content of the cross section is more than the tangential section and the radial section. The possible reason is that due to the existence of the vessels, the copper particles on the cross section are not uniformly distributed, and the local coverage is relatively high [37]. After the treatment, the surface of the poplar wood is covered with a layer of Cu nanoparticles, which contains a large number of Cu elements, which changes its surface morphology and roughness. Shirtcliffe et al. [38] used copper nanoparticles to construct a super-hydrophobic surface with a water contact angle as high as 160°. For the same surface, the more content of Cu element, the more uniform the rough surface can be obtained, so the hydrophobic performance is better [36]. For the three sections of wood, the initial surface structure is very different, which will cause the improvement effect to be inconsistent with the content of the Cu element. Since there is no copper element in the wood, the result of EDS can prove the effectiveness of HVEF treatment.

Table 1: Elements content in three section of treated poplar

	Cross section		Tangential section		Radial section	
Element	Control weight%	Treated weight%	Control weight%	Treated weight%	Control weight%	Treated weight%
C	40.66	11.64	40.33	11.47	41.03	13.96
O	59.34	10.96	59.67	15.91	58.97	14.95
Cu	0	77.4	0	66.62	0	71.09
Totals	100	100	100	100	100	100

3.2 FTIR

FTIR spectra of untreated poplar and treated poplar were obtained in Fig. 3, the marked main characteristic absorption peaks are all partially reduced. The absorption peak at 3419 cm^{-1} is caused by the stretching vibration of the hydroxyl (−OH) on the surface of the wood, which was significantly reduced. The change of the hydroxyl (−OH) group indicates that the hydrophilic group on the surface of the sample is reduced, which will affect the wettability of the wood [36]. The band at 2922 cm^{-1} is attributed to the asymmetric stretching vibration of C–H groups. The decrease in the absorption peak of C–H can also support the improvement of hydrophobic performance [39]. The C=O group in the hemicellulose corresponding to the absorption peak at 1737 cm^{-1} is significantly reduced. The reason is that the high-voltage electrostatic field stimulates the copper ion to react with the hemicellulose on the surface of the poplar wood, which causes an increase in carboxylate anions on the poplar wood surface [40]. The vibration absorption peaks at 1505 cm^{-1} corresponding to the Aromatic nucleus vibration decreased,the decrease of this absorption peak indicates that the lignin in poplar wood is also involved in the reaction [28]. The absorption peak at 1326 cm^{-1} was decreased, which means that the hydroxyl group was involved in the reaction between lignin and copper ions. The reduction of the 1246 cm^{-1} peak was caused by the Syringyl ring C–O stretching vibration and the acyl oxygen bond of hemicellulose. The absorption peak at 1168 cm^{-1} corresponding to antisymmetric bridge C–O–C stretching decreased. The

absorption peak at 1056 cm^{-1} is attributed to the C–H aromatic in-plane curve, and the absorption peak intensity is also slightly weakened. The absorption peak at 897 cm^{-1} corresponds to the decrease of C–H groups in cellulose, while the other characteristic absorption peaks of celluloses have not been significantly reduced [26]. It indicated that although the characteristic peaks of cellulose, hemicellulose and lignin on the surface of poplar wood are all weakened, the reaction still mainly happens on hemicellulose and lignin which is consistent with previous research [25].

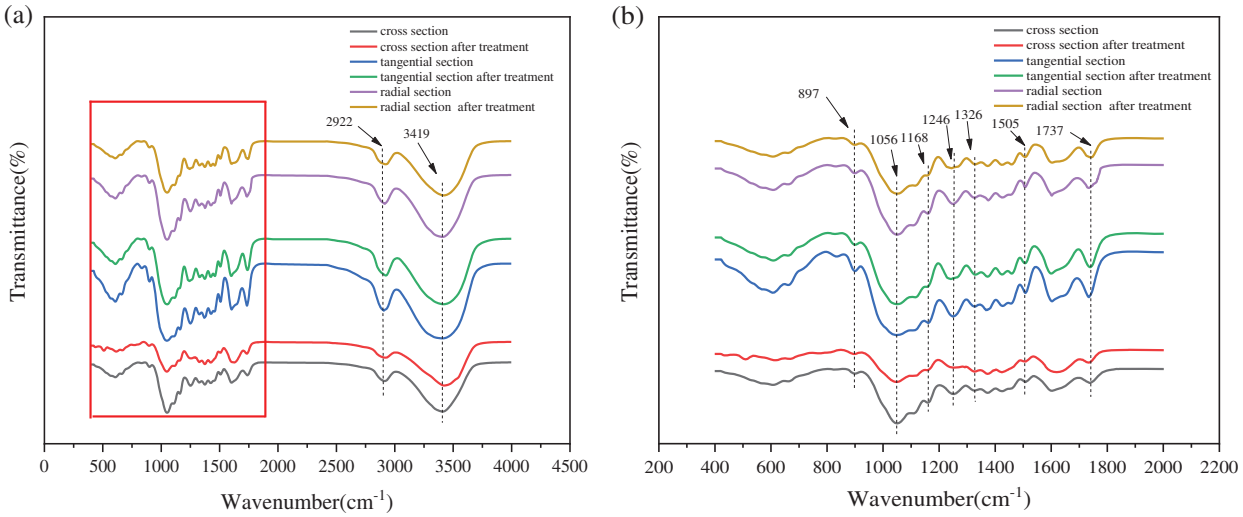

Figure 3: FTIR spectra of poplar samples and treated poplar samples: the wavenumbers of 400 to 4000 cm^{-1} (a), and 400 to 2000 cm^{-1} (b)

Table 2 shows the relative peak intensities of characteristic peaks of hemicellulose and lignin. The position of 1900 cm^{-1} is used as a standard peak which has no change after treatment. The ratio of the characteristic peaks of hemicellulose and lignin to the standard peak is the relative peak intensity mentioned. The characteristic peaks of 1737 cm^{-1} and 1246 cm^{-1} of hemicellulose and 1505 cm^{-1} and 1326 cm^{-1} of lignin are adopted to calculate. It can be seen that the decreased of characteristic peak intensity in the following order: cross section < radial section < tangential section. The spectra of the three sections of poplar have obvious differences which are closely related to the growth characteristics, wood structure and main chemical components of the wood [41]. The porosity and the low density of the cross section contribute to that the decrease of intensity of characteristic peaks being lower than that of the radial section and the tangential section.

Table 2: Comparison of relative peak intensities of characteristic peaks of hemicellulose and lignin

	Cross section			Tangential section			Radial section		
	Control	Treated	Decreased (%)	Control	Treated	Decreased (%)	Control	Treated	Decreased (%)
1326 cm^{-1}	0.75	0.76	1.14	0.38	0.53	15.40	0.63	0.70	7.71
1246 cm^{-1}	0.85	0.87	1.58	0.53	0.66	12.31	0.75	0.79	3.59
1505 cm^{-1}	0.72	0.80	8.36	0.27	0.48	21.43	0.56	0.66	10.04
1737 cm^{-1}	0.84	0.86	1.69	0.50	0.61	11.72	0.74	0.78	4.14

3.3 XRD

Fig. 4 shows the different absorption peaks before and after the treatment, It can be seen from the figure that not only new characteristic peaks are obtained after HVEF treatment, but the crystallinity of the wood cellulose is also improved. According to the JCPDS standards (Nos. 5-2872, 84-1108 and 42-0874), the peaks in the XRD pattern can be attributed to cellulose (101), cellulose(002), Cu(110), * (Peak of CuO), Cu(111), Cu(200), *, Cu(220), Cu(311), * are the peak of CuO, and the others are the peak of Cu_2O. The presence of elemental Cu, Cu_2O and CuO can be determined (The concept of phase needs to be introduced here, that is, there are phases with specific physical and chemical properties in a substance. The same element can exist in multiple or one compound states in a substance. For example, Cu element may exist in the form of elemental Cu, Cu_2O and CuO) [5]. The results show that after HVEF treatment, the reaction between the copper particles and the poplar surface composition does exist. The crystallinity of the treated poplar was significantly increased and the crystallinity of the three sections has a significantly different increase (Table 3). The possible reason for the increase is that the increase of the crystallization zone is caused by the oriented arrangement of the microfibrils which indicates that the reaction of Cu with hemicellulose and lignin which is discussed in the FTIR result affects the degree of crystalline formation of cellulose aggregates in the wood [42]. In addition, the different characteristic structures of the three sections lead to different degrees of increase in crystallinity is consistent with the result in FTIR. The degree of increase in the crystallinity of the tangential section and radial section is greater than that of the cross section, which may be due to the porous structure and lower density of the cross section.

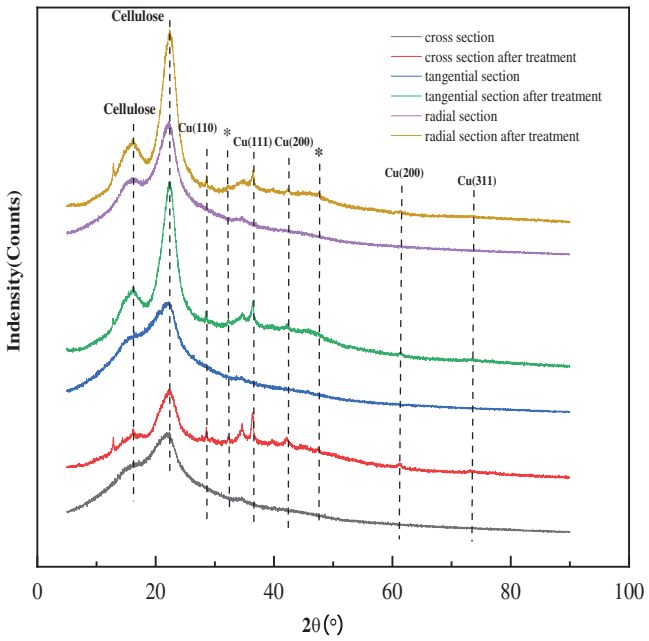

Figure 4: XRD of three section before and after treatment

Table 3: Crystallinity in three sections before and after treatment

Crystallinity	Cross section	Tangential section	Radial section
Control	29.21%	27.15%	45.32%
Treatment	46.87%	63.03%	65.54%

3.4 Wettability of Treated Poplar

Fig. 5 and Table 4 show the wettability of untreated and treated poplar wood, which is cross section, tangential section and radial section, respectively. It can be observed that the water contact angle of treated poplar (cross section, tangential section and radial section) are 121°, 157° and 143°, respectively. The results showed that the surface of treated poplars is near a superhydrophobic state, which means the treatment had a great influence on the hydrophobic state of the poplar surface. It can also be seen that with the increase in the voltage intensity, the contact angle of each section increases. The three sections of treated poplar (cross section, tangential section and radial section) were increased by 34°, 53° and 45° respectively after treatment. It gets the best processing effect at 60 kV which is consistent with the previous research [25,26]. Similar literature has reported that as the processing voltage increases, copper particles with smaller diameters and more uniform distribution will be obtained [43,44]. The increase of cross section angle is smaller, and the increase of tangential section angle and radial section angle is obvious, which means that there are differences in the treatment effect of the three sections. This difference in hydrophobic properties of different sections is caused by the special surface morphology of the wood surface such as roughness and porous structure. The characteristics of the wood tangential section and radial section are concave cell cavity ducts and ridged cell wall protrusions. The combination of the two forms the initial rough structure of the wood surface. Wood cell wall pits and ray parenchyma cells further increase the wood's surface roughness [30]. Since the cross section of poplar has many vessels, its porosity is relatively large, while the fiber voids in the tangential and radial sections are relatively small. Amorim et al. [45] reported the difference between the radial and tangential sections of the wood contact angle, and the results showed that the radial surface exhibits better wettability with water among the tested wood samples. Based on the difference in the structure of the wood itself, the increase in the contact angle of the treated poplar surface is also different which is consistent with the result in FTIR.

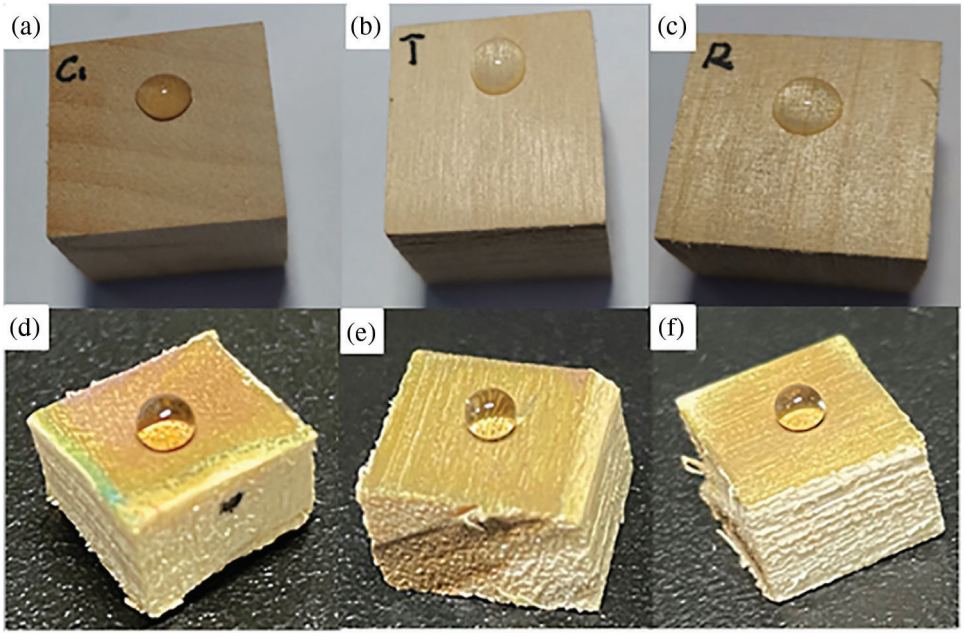

Figure 5: Wettability of cross section, tangential section and radial section of treated poplar before (a, b, c) and after (d, e, f) treatment

Table 4: Wettability of treated poplar

Wetted contact angle	Cross section	Tangential section	Radial section
Control	87°	104°	98°
20 kV	91°	109°	105°
40 kV	106°	135°	125°
60 kV	121°	157°	143°

4 Conclusion

In this study, hydrophobic poplar was prepared via HVEF with copper as the electrode plate. The results of SEM showed that a large number of copper particles were uniformly attached to the surface of poplar. In all three sections, the newly-emerged Cu element has a high weight percentage after treatment, accounting for more than half. FTIR analysis confirmed that the reaction mainly happens on hemicellulose and lignin of poplar wood, the main characteristic peaks of the three sections have different degrees of decrease. From the results of the relative peak intensities of hemicellulose and lignin, the copper particles have a higher degree of reaction with the functional groups of the tangential section. The diffraction peaks of copper-containing compounds appeared in the (XRD), copper ions with the forms of Cu(110), Cu(111), Cu(200) and Cu(311) react with poplar functional groups under HVEF treatment. The crystallinity of the cellulose of different sections has different increases, the tangential section has the greatest increase. The water contact angle of the treated poplar (cross section, tangential section and radial section) are 121°, 157° and 143°, respectively. Different increased degrees in the following order: cross section < radial section < tangential section (increased by 34°, 45° and 53°, respectively). With the increase in the voltage intensity, the contact angle of each section increases and gets the best processing effect at 60 kV. This is a simple, efficient and environmentally friendly method to modify poplar wood and expand its potential for outdoor applications.

Acknowledgement: All authors contributed equally to this work.

Funding Statement: The authors received no specific funding for this study.

Conflicts of Interest: The authors declare that they have no conflicts of interest to report regarding the present study.

References

1. Yang, X. F., Han, Y. L. (2011). Efficient utilization of poplar resources. *Wood Processing Machinery, 22,* 36–38 (in Chinese). DOI 10.3969/j.issn.1001-036X.2011.05.012.
2. Rosu, L., Varganici, C. D., Mustata, F. R., Rusu, T., Rosu, D. et al. (2018). Enhancing the thermal and fungal resistance of wood treated with natural and synthetic derived epoxy resins. *ACS Sustainable Chemistry & Engineering, 6(4),* 5470–5478. DOI 10.1021/acssuschemeng.8b00331.
3. Yue, K. (2008). *Study on the mechanical properties and durability of fast-growing poplar modified timber (Ph.D. Thesis).* Nanjing Forestry University, China.
4. Hill, C. A. S. (2011). Wood modification: An update. *Bioresources, 6(6),* 918–929. DOI 10.5552/drind.2011.1106.
5. Humar, M., Krzisnik, D., Lesar, B., Thaler, N., Ugovsek, A. et al. (2016). Thermal modification of wax-impregnated wood to enhance its physical, mechanical, and biological properties. *Holzforschung, 71(1),* 57–64. DOI 10.1515/hf-2016-0063.

6. Pori, P., Vilcnik, A., Petric, M., Skapin, A. S., Mihelcic, M. et al. (2016). Structural studies of TiO_2/wood coatings prepared by hydrothermal deposition of rutile particles from $TiCl_4$ aqueous solutions on spruce (Picea Abies) wood. *Applied Surface Science, 372(30),* 125–138. DOI 10.1016/j.apsusc.2016.03.065.
7. Yao, Y., Gellerich, A., Zauner, M., Wang, X., Kai, Z. (2018). Differential anti-fungal effects from hydrophobic and superhydrophobic wood based on cellulose and glycerol stearoyl esters. *Cellulose, 25(2),* 1329–1338. DOI 10.1007/s10570-017-1626-x.
8. Jiang, J., Chen, Y. P., Cao, J. Z., Mei, C. T. (2019). Study on the hydrophobicity of acrylic/paraffin blend emulsion treatment materials. *Forest Products Industry, 46(2),* 9–13 (in Chinese). DOI 10.19531/j.issn1001-5299.201902002.
9. Pan, Q. (2015). *Pretreatment of poplar fiber and optimization of enzymatic hydrolysis process (Master Thesis)*. Central South University of Forestry and Technology, China.
10. Chen, R. Y., Hu, G. N. (2005). Research on the densification of fast-growing poplar. *Journal of Fujian Agriculture and Forestry, 34(3),* 324–329 (in Chinese). DOI 10.3321/j.issn:1671-5470.2005.03.012.
11. Liu, F., Wang, C. Y. (2016). Wood biomimetic superhydrophobic functionalized preparation method. *Science & Technology Review, 34(19),* 120–126 (in Chinese).
12. Liu, M., Wu, Y. Q., Qing, Y., Tian, C. H., Jia, S. S. et al. (2015). Research progress of wood biomimetic superhydrophobic functional modification. *Functional Materials, 46(14),* 14012–14018 (in Chinese).
13. Wang, S., Liu, C., Liu, G., Ming, Z., Jian, L. et al. (2011). Fabrication of superhydrophobic wood surface by a sol-gel process. *Applied Surface Science, 258(2),* 806–810. DOI 10.1016/j.apsusc.2011.08.100.
14. Gao, L. K., Gan, W. T., Xiao, S. L., Zhan, X. X., Li, J. (2016). A robust superhydrophobic antibacterial Ag-TiO_2 composite film immobilized on wood substrate for photodegradation of phenol under visible-light illumination. *Ceramics International, 42(2),* 2170–2179. DOI 10.1016/j.ceramint.2015.10.002.
15. Bente, M., Avramidis, G., Forster, S., Rohwer, E. G., Viol, W. (2004). Wood surface modification in dielectric barrier discharges at atmospheric pressure for creating water repellent characteristics. *Holz Als Roh-Und Werkstoff, 62(3),* 157–163. DOI 10.1007/s00107-004-0475-0.
16. Liu, S., Liu, Q., Yi, X., Shen, Y. Z., Guo, L. et al. (2020). Investigation of heterogeneous ice nucleation on the micro-cubic structure superhydrophobic surface for enhancing icing-delay performance. *Journal of Renewable Materials, 8(12),* 1617–1631. DOI 10.32604/jrm.2020.014158.
17. Artus, G., Jung, S., Zimmermann, J., Gautschi, H. P., Seeger, S. (2010). Silicone nanofilaments and their application as superhydrophobic coatings. *Advanced Materials, 18(20),* 2758–2762. DOI 10.1002/(ISSN)1521-4095.
18. Yang, R., Liang, Y. Y., Hong, S., Zuo, S. D., Wu, Y. J. et al. (2020). Novel low-temperature chemical vapor deposition of hydrothermal delignified wood for hydrophobic property. *Polymers, 12(8),* 16. DOI 10.3390/polym12081757.
19. Yang, R., Zuo, S., Song, B., Mao, H., Xia, C. (2020). Hollow mesoporous microspheres coating for super-hydrophobicity wood with high thermostability and abrasion performance. *Polymers, 12(12),* 2856. DOI 10.3390/polym12122856.
20. Wang, F. P., Wu, H. P., Li, S., Zhang, W. G. (2017). Study on imitation of rose-like superhydrophobic structure on bamboo surface. *Journal of Bamboo, 36(3),* 49–52 (in Chinese). DOI 10.19560/j.cnki.issn1000-6567.2017.03.008.
21. Song, L., Zhang, X. F., Wang, Z. G., Bai, Y. H., Feng, Y. et al. (2020). Metal-ion induced surface modification for durable hydrophobic wood. *Advanced Materials Interfaces, 7(22),* 6. DOI 10.1002/admi.202001166.
22. Wang, K. L., Dong, Y. M., Zhang, W., Zhang, S. F., Li, J. Z. (2017). Preparation of stable superhydrophobic coatings on wood substrate surfaces via mussel-inspired polydopamine and electroless deposition methods. *Polymers, 9(6),* 12. DOI 10.3390/polym9060218.
23. Yuan, M., Hong, L., Ju, Z. H., Gu, W. L., Wang, Z. (2021). Structure design and properties of three-layer particleboard based on high voltage electrostatic field (HVEF). *Journal of Renewable Materials, 9(8),* 1433–1445. DOI 10.32604/jrm.2021.015040.

24. Kemp, B. A., Nikolayev, I., Sheppard, C. J. (2016). Coupled electrostatic and material surface stresses yield anomalous particle interactions and deformation. *Journal of Applied Physics, 119(14),* 1–7. DOI 10.1063/1.4946034.
25. Ju, Z. H., Zhan, T. Y., Zhang, H. Y., He, Q., Yuan, M. et al. (2020). Preparation of functional bamboo by combining nano-copper with hemicellulose and lignin under high voltage electric field (HVEF). *Carbohydrate Polymers, 250(24),* 116936. DOI 10.1016/j.carbpol.2020.116936.
26. He, Q., Zhan, T. Y., Zhang, H. Y., Ju, Z. H., Hong, L. et al. (2020). Facile preparation of high anti-fungal performance wood by high voltage electrostatic field (HVEF). *Journal of Cleaner Production, 260,* 120947. DOI 10.1016/j.jclepro.2020.120947.
27. Treu, A., Bardage, S., Johansson, M., Trey, S. (2014). Fungal durability of polyaniline modified wood and the impact of a low pulsed electric field. *International Biodeterioration & Biodegradation, 87(2),* 26–33. DOI 10.1016/j.ibiod.2013.11.001.
28. Chadni, M., Grimi, N., Ziegler-Devin, I., Brosse, N., Bals, O. (2019). High voltage electric discharges treatment for high molecular weight hemicelluloses extraction from spruce. *Carbohydrate Polymers, 222(13),* 115019. DOI 10.1016/j.carbpol.2019.115019.
29. Segal, L., Creely, J. J., Martin, A. E., Conrad, C. M. (1959). An empirical method for estimating the degree of crystallinity of native cellulose using the X-ray diffractometer. *Textile Research Journal, 29(10),* 786–794. DOI 10.1177/004051755902901003.
30. Hu, Y., Lu, L., Liu, J., Chen, W. (2012). Direct growth of size-controlled gold nanoparticles on reduced graphene oxide film from bulk gold by tuning electric field: Effective methodology and substrate for surface enhanced raman scattering study. *Journal of Materials Chemistry, 22(24),* 11994. DOI 10.1039/c2jm31483e.
31. Gao, L., Xiao, S., Gan, W., Zhan, X., Jian, L. (2015). Durable superamphiphobic wood surfaces from Cu_2O film modified with fluorinated alkyl silane. *RSC Advances, 5(119),* 98203–98208. DOI 10.1039/C5RA19433D.
32. Kurowska, A., Kozakiewicz., P., Borysiuk, P. (2010). An attempt at the use of laboratory density analyzer for determination of solid wood cross section density distribution. *Forestry and Wood Technology, 71(1),* 435–439. DOI 10.1.1.470.4971&rep.
33. He, Q., Zhan, T. Y., Zhang, H. Y., Ju, Z. H., Dai, C. P. et al. (2018). The effect of high voltage electrostatic field (HVEF) treatment on bonding interphase characteristics among different wood sections of Masson pine (Pinus massoniana Lamb.). *Holzforschung, 72(7),* 557–565. DOI 10.1515/hf-2017-0168.
34. Francisco, R. G., Carmen, L. D., Cinco-Moroyoqui, F. J., Josué, J., José, A. T. (2019). Preparation and characterization of quercetin-loaded zein nanoparticles by electrospraying and study of *in vitro* bioavailability. *Journal of Food Science, 84(2),* 2884–2897. DOI 10.1111/1750-3841.14803.
35. Hu, Y., Lu, L., Liu, J., Chen, W. (2012). Direct growth of size-controlled gold nanoparticles on reduced graphene oxide film from bulk gold by tuning electric field: Effective methodology and substrate for surface enhanced raman scattering study. *Journal of Materials Chemistry, 22(24),* 11994. DOI 10.1039/c2jm31483e.
36. Mu, H. B., Wang, Y. N., Tian, Y. Q., Duan, X. M., Li, J. K. et al. (2020). Microstructure and hydrophobic properties of nano-cu-coated wood-based composites by ultrasonic pretreatment. *Applied Sciences, 10(16),* 5448. DOI 10.3390/app10165448.
37. Atayde, C. M., Gonçalez, J. C., Camargos, J. A. (2011). Colorimetric characteristics of different anatomical sections of muirapiranga (Brosimum sp.) wood. *CERNE, 17(2),* 231–235. DOI 10.1590/S0104-77602011000200011.
38. Shirtcliffe, N. J., Mchale, G., Newton, M. I., Perry, C. C. (2005). Wetting and wetting transitions on copper-based super-hydrophobic surfaces. *Langmuir the Acs Journal of Surfaces & Colloids, 21(3),* 937–943. DOI 10.1021/la048630s.
39. Tapia-Hernandez, J. A., Rodriguez-Felix, D. E., Plascencia-Jatomea, M., Rascon-Chu, A., Lopez-Ahumada, G. A. et al. (2018). Porous wheat gluten microparticles obtained by electrospray: Preparation and characterization. *Advances in Polymer Technology, 37(6),* 2314–2324. DOI 10.1002/adv.21907.

40. Rodriguez-Felix, F., Del-Toro-Sanchez, C. L., Tapia-Hernandez, J. A. (2020). A new design for obtaining of white zein micro- and nanoparticles powder: Antisolvent-dialysis method. *Food Science and Biotechnology, 29(5),* 619–629. DOI 10.1007/s10068-019-00702-9.
41. Jankowska, A., Zbiec, M., Kozakiewicz, P., Koczan, G., Olenska, S. et al. (2018). The wettability and surface free energy of sawn, sliced and sanded european oak wood. *Maderas-Ciencia Y Tecnología, 20(3),* 443–454. DOI 10.4067/S0718-221X2018005031401.
42. Agarwal, U. P., Ralph, S. A., Reiner, R. S., Moore, R. K., Baez, C. (2014). Impacts of fiber orientation and milling on observed crystallinity in jack pine. *Wood Science and Technology, 48(6),* 1213–1227. DOI 10.1007/s00226-014-0667-7.
43. Rodriguez-Felix, F., Lopez-Cota, A. G., Moreno-Vasquez, M. J., Graciano-Verdugo, A. Z., Quintero-Reyes, I. E. et al. (2021). Sustainable-green synthesis of silver nanoparticles using safflower (*Carthamus tinctorius* L.) waste extract and its antibacterial activity. *Heliyon, 7(4),* e06923. DOI 10.1016/j.heliyon.2021.e06923.
44. Tapia-Hernandez, J. A., Del-Toro-Sanchez, C. L., Cinco-Moroyoqui, F. J., Ruiz-Cruz, S., Juarez, J. et al. (2019). Gallic acid-loaded zein nanoparticles by electrospraying process. *Journal of Food Science, 84(4),* 818–831. DOI 10.1111/1750-3841.14486.
45. Amorim, M. R. S., Ribeiro, P. G., Martins, S. A., DelMenezzi, C. H. S., Souza, M. R. (2013). Surface wettability and roughness of 11 amazonian tropical hardwoods. *Floresta e Ambiente, 20(1),* 99–109. DOI 10.4322/floram.2012.069.